- Machine Learning Identifies Microbiome and Clinical Predictors of Sustained Weight Loss Following
- 2 Prolonged Fasting

3

10

- 4 Gelsomina N. Kaufhold^{1,2,3,*}, Theda U. P. Bartolomaeus^{1,2,3,4,*}, Kristin Kräker^{1,2,3,4}, Till Schütte^{1,2,3,4},
- 5 Sakshi Kamboj⁵, Ulrike Löber^{1,2,3,4}, Gabriele Rahn¹, Victoria McParland^{1,3,6}, Lena Braun¹,
- 6 Lajos Markó^{1,2,3,4}, Matanat Mammadli^{1,2,3}, Alexander Krannich⁷, Lina S. Bahr^{1,2,3},
- 7 Friederike Gutmann^{1,2,3,4}, Friedemann Paul^{1,2,3}, Nicola Wilck^{1,3,4,6}, Alma Zernecke⁸, Peter J. Oefner⁵,
- 8 Wolfram Gronwald⁵, Dominik N. Müller^{1,2,3,4}, Sofia K. Forslund-Startceva^{1,2,3,4,9}, Sylvia Bähring^{1,2,3,†},
- 9 Hendrik Bartolomaeus^{3,4,8,†}, Nadja Siebert^{1,2,3,†}
- 11 ¹Experimental and Clinical Research Center (ECRC), a cooperation of Charité Universitätsmedizin
- 12 Berlin and Max Delbrück Center for Molecular Medicine, Berlin, Germany
- 13 ²Charité-Universitätsmedizin Berlin, corporate member of Freie Universität Berlin and Humboldt-
- 14 Universität zu Berlin, Berlin, Germany.
- 15 ³Max Delbrück Center for Molecular Medicine in the Helmholtz Association (MDC), Berlin, Germany
- 16 ⁴DZHK (German Centre for Cardiovascular Research), partner site Berlin, Germany
- 17 ⁵Institute of Functional Genomics, University of Regensburg, Regensburg, Germany
- 18 ⁶Department of Nephrology and Internal Intensive Care Medicine, Charité -Universitätsmedizin
- 19 Berlin, Germany.
- ⁷BioStats GmbH, Nauen, Germany
- 21 *Institute of Experimental Biomedicine, University Hospital Würzburg, Germany.
- ⁹Structural and Computational Biology Unit, European Molecular Biology Laboratory (EMBL),
- 23 Heidelberg, Germany.
- 25 *contributed equally

- 26 †jointly supervised the work
- 27 Correspondence: bartolomae h@ukw.de

Abstract

Prolonged fasting may benefit metabolic health, but data in healthy individuals remain limited. We performed a randomized, waitlist-controlled study (LEANER study), with 38 healthy participants completing a 5-day-fasting intervention with 12-week follow-up. Fasting acutely lowered body mass index (BMI), via fat mass loss. These changes partially persisted at follow-up. Fasting altered the gut microbiome composition and induced metabolite shifts in plasma and feces. Changes to gut microbiome alpha diversity after fasting correlated with baseline microbiome diversity. Long-term BMI response at follow-up could be predicted through machine learning (ML) using baseline microbiome and clinical data, highlighting an unknown *Faecalibacterium* sp., *Oscillibacter* sp. 50_27, LDL cholesterol, and systolic blood pressure as key predictors. This ML model was validated in independent patient cohorts with metabolic syndrome and multiple sclerosis. These findings support prolonged fasting as an effective metabolic intervention and demonstrate that individual responses to fasting interventions can be predicted using pre-intervention features.

Trial registration: ClinicalTrials.gov, NCT04452916. Registered on June 26, 2020

- **Key words:** fasting, gut microbiome, weight loss, machine learning, personalized nutrition,
- 46 precision medicine

Introduction

47

48

49

50

51

52

53

54

55

56

57

58

59

60

61

62

63

64

65

66

67

68

69

70

Fasting interventions have gained renewed attention for their potential to modulate metabolism, reshape the gut microbiome, and promote healthy aging¹. While fasting protocols vary widely from time-restricted eating to fasting-mimicking diets², and prolonged food abstinence lasting up to several weeks (up to 26 days)³, the underlying principle is consistent: transient caloric deprivation triggers coordinated physiological responses that may confer long-term health benefits⁴. Evidence from patient populations, including those with metabolic syndrome⁵, autoimmune diseases^{6,7}, and cancer⁸, suggests that fasting can influence key regulatory pathways such as autophagy, insulin sensitivity, and oxidative stress¹. In individuals with metabolic syndrome. we previously demonstrated that a 5-day fast atop a DASH (Dietary Approaches to Stop Hypertension) diet induced profound and coordinated changes in gut microbiome composition and immune cell states most of which were reversed at 12 weeks follow-up⁵. Using immune cell population or microbiome profiles, we developed models that predicted long-term antihypertensive effects, supporting the concept of data-driven stratification⁵. In parallel, gut microbiome profiling has emerged as a powerful tool for personalized medicine⁹. Microbial signatures have been linked to energy metabolism¹⁰, weight regulation ^{11,12}, and immune modulation ^{13,14}. Personalized dietary approaches that account for microbiome composition have demonstrated superior outcomes in metabolic control⁸. Emerging applications extend to autoimmune, neuropsychiatric, and oncologic indications, underscoring the potential of microbiome-informed strategies in precision medicine 9,15. Despite these advances, the long-term effects of prolonged fasting in healthy individuals remain poorly characterized. Most existing studies rely on non-randomized designs, lack adequate control groups, or fail to include follow-up assessments. Furthermore, many

interventions are performed in multimodal clinical settings involving exercise, psychological support, and dietary coaching⁵, making it difficult to isolate the effect of fasting alone.

Here, we present a randomized, waitlist-controlled study investigating the effects of a 5-day prolonged fasting intervention in healthy adults, with follow-up assessments at 12 weeks. We integrated clinical, microbiome, and metabolome profiling to characterize immediate and long-term physiological responses. Using machine learning, we show that sustained weight loss can be predicted from baseline microbiome and clinical features. The results that were validated in independent cohorts with metabolic syndrome and multiple sclerosis. Our findings offer mechanistic insight into fasting responses and support the potential of microbiome-informed strategies for personalized lifestyle interventions.

Results

82

83

84

85

86

87

88

89

90

91

92

93

94

95

96

97

98

99

100

101

102

103

104

105

Prolonged fasting affects energy expenditure and long-term weight loss Thirty-eight healthy participants were recruited for a 5-day prolonged fasting intervention (Figure 1a). As fasting interventions cannot be blinded, we decided to use a waiting list control to account for physiological fluctuations within a 12-week timeframe while maximizing the number of participants undergoing prolonged fasting (Figure 1A). Baseline characteristics are shown in Table 1. Of the 38 participants, 83% reported fasting-related adverse events (AE) (Table S1). All AE were mild and transient and did not necessitate discontinuation of fasting. Blood glucose and β-hydroxybutyrate levels were measured each morning and evening during the five-day fasting period (days 1-5), confirming that all participants adhered closely to the study protocol (Figure S1a, b). We observed a diurnal rhythm with higher BHB but lower glucose concentrations in the morning compared to the evening (Figure S1a, b). Continuous interstitial glucose monitoring during the five-day fasting period, compared with baseline measurements and waiting-list controls, confirmed a dynamic reduction in glucose levels over the course of the fast. (Figure 1b). Following refeeding the glucose levels normalized; however, between days 2 and 4 post-fast, blood glucose concentrations were elevated throughout the day (06:00-22:00) compared with baseline measurements (Figure 1c). Our predefined endpoint was a change in resting energy expenditure (REE). Prolonged fasting acutely reduced REE by 62 kcal/d, suggesting a fasting-induced, energy-preserving mechanism (Figure 1d, Supplementary Data 1). We did not observe alterations in REE between the two baseline timepoints of waiting list controls (Figure 1d). Since REE was the defined endpoint, we performed a linear mixed model showing that lean mass (p < 0.001)

and not self-reported sex significantly influenced REE at all visits, including post-fasting

107

108

109

110

111

112

113

114

115

116

117

118

119

120

121

122

123

124

125

126

127

128

129

(Figure S2). Following the five-day fast, respiratory exchange ratios (RER) declined significantly (Figure 1e), paralleling a peak in BHB concentrations on day 5 (Figure S1b). All those metabolic makers returned to baseline by 12 weeks post-fast. Furthermore, we observed that prolonged fasting reduced BMI (Figure 1f). This decrease was partly reversed after 12 weeks follow-up (Figure 1f). Body composition analysis attributed this incomplete return towards baseline BMI predominantly to a reduction in fat mass (Figure 1g, S1g). Of note, the absolute and relative reduction of body fat was accompanied by a reduction in lean mass during fasting that completely reverted at follow-up (Figure S1h). Prolonged fasting reduced waist-to-hip ratio and diastolic blood pressure while increasing heart rate, findings which are consistent with a previously published study in metabolic syndrome (Figure S1d-g). In contrast to metabolic syndrome patients⁵, the healthy participants in this study did not exhibit sustained blood-pressure reductions (Figure S1e, f). Taken together, these results demonstrate that prolonged fasting is well tolerated in healthy individuals, yielding sustained reductions in BMI and fat mass, while most metabolic and hemodynamic parameters return to baseline during the 12-week follow-up. Prolonged fasting induces large short-term and small long-term changes in gut microbiome composition To assess the natural fluctuation of the gut microbiome composition, we analyzed changes between the two baseline samples (baseline 0 and baseline 1) from the waiting list control (Figure 1a). Microbial alpha diversity, measured as Shannon index, and microbiome composition quantified by Bray-Curtis dissimilarity did not differ significantly between the two baseline samples (Figure S3a, b). Shannon index remained stable across all study visits (Figure 2a). In contrast, individual trajectories in response to fasting varied markedly (Figure

131

132

133

134

135

136

137

138

139

140

141

142

143

144

145

146

147

148

149

150

151

152

153

2a). Interestingly, short-term (post-fasting) and long-term (follow-up) changes in alphadiversity correlated negatively with alpha-diversity at baseline, implicating baseline differences in microbiome composition as relevant predictors of fasting-induced microbiome changes (Figure 2b, c). Bray-Curtis dissimilarity-based multivariate analysis of the taxonomic composition demonstrated a significant shift in microbial community composition in response to fasting that partially reversed during the follow-up period (Figure 2d). Consistent with the observed shift in the multivariate analysis, fasting induced significant changes in several bacterial species that reversed during follow-up. For example, Roseburia sp. inserta sedis and Bifidobacterium adolescentis decreased after the fasting period but increased at follow-up, whereas Faecalibacterium sp. CAG-74 showed the opposite pattern (Figure 2e, S3c, Supplementary Data 2). In contrast, only seven taxa exhibited sustained abundance changes (Figure S3c). Next, we analyzed gut-specific metabolic modules using GOmixer. Again, fasting induced pronounced alterations that largely reverted to baseline during follow-up (Figure 2f). Only for three modules. ketone body synthesis, osmoprotectant transport system, and N-acetylneuraminate and N-acetylmannosamine degradation, fasting induced a long-lasting increase when comparing baseline to follow-up (Figure 2f, Figure S4a, Supplementary Data 3). Overall, prolonged fasting induces pronounced compositional shifts in the gut microbiome which were largely reversed upon refeeding, resulting in minimal long-term deviations from baseline at the 12-week follow-up. Notably, baseline alpha diversity metrics correlate with the magnitude of alpha diversity changes both immediately after fasting and at follow-up.

Prolonged fasting alters plasma and fecal metabolome

155

156

157

158

159

160

161

162

163

164

165

166

167

168

169

170

171

172

173

174

175

176

177

We performed nuclear magnetic resonance (NMR) spectroscopy on plasma and fecal samples to assess the impact of fasting, and its associated microbiome shifts on the fecal and host metabolome. Principal coordinate analysis (PCA), centered on baseline values to characterize post-fast changes and on post-fast values to characterize follow-up effects, revealed plasma metabolome trajectories analogous to those observed in the gut microbiome (Figure S4b). In line, we observed significant alterations between baseline, fasting, and follow-up, with most changes reversed at follow-up (Figure S4c, Supplementary Data 4). In plasma, only valine, glycine, tyrosine, and pyruvic acid exhibited sustained increases from baseline to follow-up, indicating lasting effects of fasting on these metabolites (Figure S4b, c). Fecal metabolite profiling again revealed a pattern of alteration and reversion to baseline (Figure S4d). Contradicting other previous reports on short-chain fatty acids (SCFA) in fasting⁵, we observed a decrease in butyrate during fasting, which was non-significant at follow-up (Figure S4e, Supplementary Data 5). The only long-term effect observed in our data was a decrease in choline from baseline to fasting (Figure S4e). In conclusion, NMR-based metabolomics of plasma shows more consistent alterations as compared to the fecal metabolome, which might be due to the different matrix or intraindividual variations in gut microbiome composition.

Prediction of sustained BMI response by multi-omics machine learning

Since we observed strong intraindividual differences in response to prolonged fasting across most data layers, we aimed to investigate whether the clinical response to fasting can be predicted from baseline data. Since BMI showed the overall strongest long-term effect of the analyzed clinical data (Figure 1), we focused on the long-term weight loss phenotype. Using

179

180

181

182

183

184

185

186

187

188

189

190

191

192

193

194

195

196

197

198

199

200

the waiting list control, we estimated the normal fluctuation of BMI within 12 weeks of study participation. Normal fluctuation in BMI was defined as mean ± two standard deviations $(SD)^{16}$, in our case -0.008 ± 0.32 kg/m². With this threshold, we identified 38% BMI long-term responders and 62% BMI non-responders to prolonged fasting. In order to cross-validate our model in publicly available datasets we focused on microbiome and clinical features over NMR metabolomics^{5,17}. A random forest classifier was trained on 87 features including the 50 most abundant species, candidate species and pathways from previous studies on prolonged fasting, as well as relevant clinical metadata (Supplementary Data 6) using 80% of our data. To account for the small sample size, we used leave-one-out cross-validation. The model was evaluated on the remaining 20% of the dataset that was held out during training (Figure 3a). The initial model achieved 66.7% accuracy with 100% sensitivity in identifying responders in the test dataset. To optimize performance, we then selected key predictors using randomforest feature importance, the Boruta algorithm, and backward feature elimination (Figure 3b, S5c). This analysis indicated four key predictors: LDL, systolic blood pressure (BP), Faecalibacterium sp. incerta sedis and Oscillibacter sp. 57 20. Those four features were used to train the final model on 80% of the dataset. The refined model demonstrated improved performance, achieving 83.3 % accuracy, an 80% positive predictive value, and a 100% negative predictive value (Figure S5a). Baseline BMI can confound weight loss predictions, so we tested for collinearity and correlations between baseline BMI and our four selected features none of which reached significance (Figure 3c). To further test if our four features are mere surrogate markers of baseline BMI, we incorporated baseline BMI into the model which did not improve predictive accuracy (Figure S5b). Furthermore, Oscillibacter sp. 57 20 remained the most important

202

203

204

205

206

207

208

209

210

211

212

213

214

215

216

217

218

219

220

221

222

223

224

feature. These results confirm that our final model captured biologically relevant signals beyond simple baseline BMI effects. Finally, we examined the abundance patterns of the model's key features within our cohort. Responders exhibited significantly higher levels of Oscillibacter sp. 57 20 (Figure 3d), while the identified Faecalibacterium sp. showed no significant difference (Figure 3f). Although important for responder identification, we observed no significant differences in systolic blood pressure or plasma LDL levels between responders and non-responders (Figure 3e, g). Taken together, we identified four (two clinical and two microbiome) features that hold the potential to predict long-term weight loss in response to prolonged fasting interventions. Although our model performed robustly on the 20 % hold-out set, these results were achieved in a very limited cohort size. Validation in available datasets of patients with co-morbidities To address this limitation, we next applied our model to our published metabolic syndrome cohort in which patients underwent either a five-day fasting regimen followed by a DASH diet or a DASH diet alone (Figure 4a)⁵. The study outcomes were assessed 12 weeks postintervention, mirroring our study's timeline. Given the greater BMI variability expected in metabolic syndrome patients, we again quantified BMI fluctuation from the DASH only group and subsequently defined long-term responders with a BMI reduction exceeding 0.8 kg/m². Remarkably, our trained model predicted sustained weight loss in this study with an AUC of 0.85 (Figure 4b). Our model correctly classified 19 (82.6% [61.2 – 95.1%] accuracy) of the 23 patients and with a sensitivity and specificity of 85.7 % and 81.3 %, respectively (Figure 4b). Furthermore, patients classified as responders showed a significantly higher BMI reduction at

12 weeks follow-up compared to non-responders (Figure 4c, d). Consistent with our

healthy-participant cohort, the model's predictive features exhibited only weak correlations with baseline BMI, underscoring their independence from initial body mass (Fig. 4e). In univariate analyses, none of the features differed significantly at baseline between responders and non-responders (Figure 4f-i). As further validation, we selected a recent nutritional intervention trial in multiple sclerosis patients, the majority of whom exhibited normal metabolic profiles (obesity in one patient, hypertension in two patients, high LDL in four patients) ¹⁷. Notably, the study design differed substantially. Patients completed two prolonged fasting cycles, interspersed with an interim period of intermittent fasting (14 hrs/day), and follow-up assessments were conducted nine months apart (Figure 5a). As the control arm of this study included dietary counseling, following the dietary recommendations of the German Society of Nutrition, we did not use it to define average BMI shifts over nine months. Therefore, we could not calculate specificity or sensitivity. Nevertheless, patients classified as responders by our model experienced significantly greater weight loss than those classified as non-responders (Figure 5b). Again, no significant correlations between model parameters and baseline BMI were detected in this cohort (Figure 5c). Similar to the current cohort, levels of Oscillibacter sp. 50 27 were significantly higher in responders (Figure 5e. The other features did not differ significantly (Figure 5f-h). Our findings indicate that baseline patient characteristics determine the magnitude of longterm weight response to prolonged fasting interventions. Furthermore, the predictive model, initially developed in healthy subjects, retained robust performance when applied to both individuals with metabolic syndrome and to a regimen involving two separate prolongedfasting episodes.

225

226

227

228

229

230

231

232

233

234

235

236

237

238

239

240

241

242

243

244

245

246

Metabolite associations with Oscillibacter sp. 57_20 and Faecalibacterium sp. incertae sedis

Since both the Oscillibacter sp. 57_20 and the Faecalibacterium sp. identified in this study were predictive of weight loss, we wanted to further understand the potential metabolite profile associated with these bacteria. Therefore, we performed an exploratory correlation analysis with the fecal metabolome across all visit data while blocking the visit information¹⁸. We found significant associations of Faecalibacterium sp. with butyrate, tryptophan, and uridine (Figure 6a-c, Supplementary Data 7) as well as of Oscillibacter sp. 57_20 with glycerol and methionine, and for uridine without reaching statistical significance (Figure 6d-f, Supplementary Data 8). In summary, our data suggest that the bacterial species important for the classification of long-term body weight responders modulate the metabolomic output of the fecal microbiome.

Discussion

261

262

263

264

265

266

267

268

269

270

271

272

273

274

275

276

277

278

279

280

281

282

283

284

Our data show that prolonged fasting leads to long-term body weight and body fat reduction after 12 weeks. Interindividual variability in response to dietary interventions poses a major challenge in lifestyle interventions. Large-scale studies have shown that both host and microbial factors shape individual metabolic responses, emphasizing the need for precision strategies ^{19,20}. Using baseline microbiome and clinical data, we can predict individuals who will respond to fasting with sustained weight loss, defined as a BMI reduction lower than the mean minus two standard deviations of the waiting list control. Using available data from similar interventions in patients with metabolic syndrome and patients with multiple sclerosis, we could validate our data-driven classification approach. While Faecalibacterium sp. incertae sedis and Oscillibacter sp. 57 20, were important for BMI response prediction, most of the microbiome and metabolome features were characterized by transient shifts induced by fasting, with subsequent return to pre-intervention states. Taken together, our data implicate gut microbiota in long-term BMI changes post fasting and suggest conserved effects of fasting regardless of health status. On host level, prolonged fasting led to strong changes of multiple cardiometabolic risk factors like LDL cholesterol, waist-to-hip ratio, and systolic and diastolic blood pressure. However, at 12 weeks follow-up these changes mainly reverted, indicating that prolonged fasting does not exert a sustained effect in healthy individuals. These data differ from in patients with metabolic syndrome with values above the healthy range⁵. Interestingly, while blood glucose dropped during fasting, it increased upon refeeding during the day (6am to 10pm). Since values at night (10pm to 6am) did not increase, our data suggest a mildly disturbed glucose handling for the early days post-fasting. A similar phenotype was reported in the literature in response to standardized meal intakes after prolonged fasting^{21,22}. This was attributed to the

286

287

288

289

290

291

292

293

294

295

296

297

298

299

300

301

302

303

304

305

306

307

308

metabolism successfully switching to fatty acid and ketone oxidation and postprandial carbohydrate oxidation was reduced leading to higher plasma glucose levels²¹. Since a strong metabolic phenotype was expected, REE reduction was our predefined endpoint. REE in fasting was studied previously mainly in healthy men²³⁻²⁵ Our data shows an overall similar but smaller effect, which might be due to the inclusion of healthy women and a broader range of lean masses. Levels of REE reduction after 24h caloric deprivation was previously associated with weight gain after 6 months in healthy individuals²⁶. We could not confirm these findings in our cohort for long-term weight changes after 3 months using the changes in REE after 5 days of fasting (Figure S6). However, using a combination of clinical and microbiome data, we were successful in predicting long-term weight loss. We have shown in the past the microbiome and immune data can predict blood pressure reduction in patients with metabolic syndrome in response to fasting⁵. In contrast, our study in healthy participants revealed only modest effects on blood pressure. Given the wellestablished impact of fasting on weight managemen²⁷, we applied a data-driven approach that involved clustering participants based on BMI changes and employing a random forest classifier. Our initial model, which incorporated 83 features, demonstrated high sensitivity but limited specificity, iterative feature selection enabled us to identify Faecalibacterium sp. incertae sedis, Oscillibacter sp. 57 20, plasma LDL levels, and systolic blood pressure as key predictors. Notably, independent validations highlighted the robustness and generalizability of our approach. In the Maifeld et al. cohort⁵, which featured a similar study design in patients with metabolic syndrome, we observed an 82.6% of responders were correctly identified. In the Bahr et al. cohort¹⁷, with a different study design incorporating intermittent fasting in patients with multiple sclerosis, predicted responders exhibited higher weight loss. These external validations not only reinforce the reliability of our predictive model but also

310

311

312

313

314

315

316

317

318

319

320

321

322

323

324

325

326

327

328

329

330

331

suggest that the gut microbiome changes associated with fasting responses are conserved across diverse populations, from healthy individuals to those with metabolic disorders and autoimmune disease, thereby broadening the potential applicability of fasting-based interventions for weight management and metabolic health. Given that baseline BMI is typically a key predictor of weight loss, we assessed its confounding effect on fasting-induced BMI changes. Oscillibacter sp. 57 20 remained the stronger predictor even when baseline BMI was included in the model, indicating that this microbial species may exert an independent influence on weight regulation during fasting. While we cannot fully exclude potential confounding or correlations between baseline BMI and microbiome composition, to our knowledge, no prior study has directly linked Oscillibacter sp. 57 20 with weight regulation. However, Oscillibacter sp. 57 20 was recently identified as a keystone taxon in a similar prolonged fasting study in healthy individuals, where it was implicated in the production of indole-3-propionate (I3P)²⁸, a protective metabolite in cardiometabolic disease²⁹. Future research is needed to explore the mechanistic role of Oscillibacter spp. in host metabolism and its potential relevance in personalized fasting interventions. Faecalibacterium spp. are known SCFA producers³⁰. In line, our data shows that the abundance of our specific Faecalibacterium sp. associates with fecal butyrate levels. As described previously for other Faecalibacterium spp. 31, the identified Faecalibacterium sp. correlates with fecal tryptophan. Tryptophan can be catabolized by gut microbiota to indole metabolites³². Unfortunately, due to the resolution of NMR metabolomics, we could not detect specific indole metabolites like I3P. However, our data implicate that both bacteria might interact in the production of tryptophan catabolites.

333

334

335

336

337

338

339

340

341

342

343

344

345

346

347

348

349

350

351

352

353

354

355

Both the Faecalibacterium sp. identified in this study and the Oscillibacter sp. 57 20 correlate with the nucleoside uridine. Uridine can adaptively regulate food intake in healthy participants³³. Furthermore, experimental evidence show that blood uridine levels reflect the nutritional status of mice^{34,35} with high uridine levels as indicators of catabolic states^{34,36}. In line, dietary supplementation of uridine enhanced hunger and increased caloric intake³³. Microbial metabolism of uridine suggests a potential role of a gut-brain axis or influence on satiety³⁷ in long-term BMI responders. Unfortunately, the literature concerning the other metabolites of interest correlating with Oscillibacter sp. 57 20, glycerol and methionine is sparse. While we controlled our analysis for abundance shifts at different visits, we could not control the false discovery rate in this exploratory setting. Future confirmatory studies are needed to further investigate the metabolite spectra of the identified Faecalibacterium sp. and Oscillibacter sp. 57 20. Overall, the gut microbiome and metabolome exhibited a consistent pattern of fastinginduced alterations and nearly complete reversion to baseline at follow-up. Previous studies have consistently reported an enrichment of beneficial bacteria such as F. prausnitzii 38-40, as well as Roseburia and Coprococcus species, other known SCFA producers 41-43. Our data only partly overlaps with these reports, as we observed no alterations to F. prausnitzii, alongside a decrease in Roseburia spp. and Coprococcus spp. However, we observed an increase in one Butyricicoccus sp., known butyrate producers. Our functional analysis revealed an increase in propionate production via kinase pathways, pointing towards an elevated SCFA production potentials from coordinated activity across broader microbial community rather than single species effects. The discrepancy with earlier findings may be attributed to our study's healthy cohort, in which baseline levels of F. prausnitzii are likely already well-balanced. This suggests that fasting might predominantly restore disturbed bacterial populations rather than altering

357

358

359

360

361

362

363

364

365

366

367

368

369

370

371

372

373

374

375

376

377

378

379

already stable communities. Suggest that fasting primarily restores imbalanced microbial populations, rather than reshaping already stable communities. 44 Interestingly and consistent previous studies, we did not observe overall change in alpha diversity^{5,42}. However, participants with lower baseline alpha diversity responded with a long-lasting increase to the fasting intervention. High microbial diversity stabilizes microbiota functions during perturbations⁴⁵. In diseases usually associated with lower alpha diversity, such as obesity, other fasting interventions increase alpha diversity 46. Together, these studies reinforce the hypothesis that fasting effects on alpha diversity are more pronounced in individuals with a reduced microbial diversity. However, low baseline alpha diversity may also arise from unaccounted external influences (e.g., lifestyle habits immediately preceding the measurement). Despite these promising results, our study has several limitations. First, the lack of comprehensive documentation on dietary intake following the fasting intervention. Whether significant weight loss was solely due to fasting or also influenced by subsequent dietary modifications, a common limitation in caloric restriction studies, cannot be determined. From a computational perspective, the relatively small sample size, particularly the initial test dataset after splitting, poses challenges for the random forest model and feature selection⁴⁷. However, the validation in two independent cohort shows the robustness of our approach⁴⁸. In conclusion, our study provides compelling evidence that fasting induces substantial yet reversible changes in the gut microbiome and host metabolic profiles. Importantly, a subset of individuals experiences sustained weight loss. The integration of microbial and clinical data not only enhanced our predictive capabilities but also unveiled novel associations, such as the independent role of Oscillibacter sp. 57 20 and Faecalibacterium sp. incertae sedis in weight regulation. Despite limitations related to dietary documentation and sample size,

these findings pave the way for future research aimed at refining personalized fasting interventions. Ultimately, our work underscores the promise of leveraging gut microbiome insights to tailor dietary strategies for improved metabolic health and weight management.

Methods

Study design

We performed a randomized, waitlist-controlled study (LEANER study, ClinicalTrials.gov; NCT04452916) carried out at the Experimental and Clinical Research Center of Charité – Universitätsmedizin in Berlin, from November 2020 to December 2022. The study protocol was approved by the institutional review board of Charité – Universitätsmedizin Berlin (EA1/033/20) and all participants provided written informed consent before entering the study. We collected and managed study data using REDCap electronic data capture tools hosted at Charité – Universitätsmedizin Berlin^{49,50}. This study was exploratory, and we did not calculate a pre-determined sample size. Instead, the size of the recruited cohort was determined based on methodological and feasibility considerations. A general overview of the study is provided in Fig. 1a.

Eligibility criteria

We included individuals aged 20-50, who were assigned male or female at birth and identified as men and women, respectively; with a body mass index between 20-30 kg/m². Exclusion criteria were heart, lung, liver, and kidney diseases requiring medical intervention, prescribed medication (except oral contraceptives), postoperative phases, current or chronic infection, antibiotic treatment or a fasting week within the last 6 months, habitual use of dietary supplements, food intolerances, > 2 kg body weight change within the last month, pregnancy, lactation, vegan diet, smoking, drug, or alcohol abuse.

Intervention

Participants received oral and written instructions on the method of prolonged fasting. Expert guidance was provided by experienced nutritionists and certified fasting counselors in a group setting with 5-10 participants per group. After sufficient instruction, the fasting was performed individually at home, with the possibility of reaching out to the counselor at any time or to connect with other group members (if patients gave consent to share this information). Participants were encouraged but not required to take time off during this week. Fasting was preceded by one preparation day, on which participants consumed a low-calorie, fiber-rich diet, e.g. fruits, vegetables, potatoes, rice, oats.

During the five fasting days, participants were allowed to consume 200-250 kcal/d through vegetable juices and vegetable broths. Herbal teas and water could be consumed ad libitum.

At the morning of fasting day 6, we performed the study visit and patients were instructed for the refeeding phase. A detailed fasting plan including refeeding recommendation is provided as Supplementary Table S2.

Randomization

We assigned participants randomly according to a locked list created by www.randomizer.at (two treatments: waiting, fasting; 1 factor: self-reported sex; permuted blocks; block sizes 4, 2, 6, 4). Due to the nature of the intervention and the wait-list design, blinding was not possible.

Outcome measures

We established all outcome measures in advance and did not adapt them during or after the study. The primary outcome measure was resting energy expenditure (REE in kcal/d) after 5 days of fasting vs. baseline 1 assessed by indirect calorimetry. Secondary outcomes were

body composition, cardiovascular parameters, various routine blood parameters, glucose variability, gut metagenome, fecal and plasma metabolome. In addition, we assessed compliance and safety of fasting.

Study center assessments

431

432

433

434

435

436

437

438

439

440

441

442

443

444

445

446

447

448

449

450

451

452

The waiting group underwent assessments four times, the fasting group three times. The fasting group had one baseline visit (baseline 1) and started the intervention within two to eleven days afterwards, the waiting group had two baseline visits with a 12-week waiting period in between (baseline 0 and baseline 1) and also started the intervention within a maximum of 11 days after baseline 1. These two baselines allowed detection of random time effects on the assessed outcome measures. For both groups, the next visit was on the morning of the sixth fasting day directly before breaking the fast (fasting). To assess mediumterm effects of fasting, there was another visit after 12 weeks (follow-up). Except for the additional baseline 0 in the waiting group, all assessments were identical between the groups. All examinations described hereafter were performed at all study visits. Assessments commenced in the morning following a 12-hour overnight fast. Participants were instructed to abstain from caffeine, alcohol, and vigorous exercise for 24 hours prior to the assessments. Venous blood was drawn and sent to an accredited laboratory (Labor Berlin, Berlin, Germany) that measured parameters of glucose and lipid metabolism, blood count, electrolytes, liver enzymes, uric acid, CRP, and renal function according to international standards.

454

455

456

457

458

459

460

461

462

463

464

465

466

467

468

469

470

471

472

473

474

475

476

We measured waist and hip circumference to calculate waist-to-hip ratio and determined body composition (lean and fat mass) by air displacement plethysmography (Bod Pod, Life Measurements, Inc., Concord, CA). Indirect calorimetry was conducted following a 30 min resting period while in a supine position within a thermoneutral environment for a duration of 30 min (Quark RMR, COSMED, Italy). REE and respiratory exchange ratio (RER) were calculated from oxygen consumption and carbon dioxide production as described elsewhere. 51 Office blood pressure and heart rate were determined by five automated measurements within 10 min with an upper arm cuff (Mobil-o-Graph, I.E.M. GmbH, Stolberg, Germany) in the absence of study personnel. **Fecal samples** At each study visit, participants received two stool collection kits and were asked to collect two samples from one stool at home as soon as possible following the study visit. One sample was used for gut metagenome sequencing (OMNIgene Gut, DNA Genotek, Ottawa, Canada) and the other for metabolome analysis (OMNImet Gut, DNA Genotek, Ottawa, Canada). These kits allow shipment without cooling to the study center. Participants sent the tubes to the study center at room temperature, where they were stored at -80°C until further processing. **Glucose sensors** We assessed glucose variability by continuous glucose monitoring over 14 days. For this, participants wore a glucose sensor that measured interstitial glucose concentrations in the

subcutaneous tissue of the dorsal upper arm every 15 min (FreeStyle Libre Pro, Abbott,

Chicago, IL, USA). In contrast to the use of these sensors in diabetic patients, participants in this study could not see their values during the measurement. Baseline assessment was done only in the waiting group directly following baseline visit 0. Additionally, fasting assessment was done in all participants during preparation, fasting and refeeding.

Ketone and glucose measurements

On the five fasting days, participants independently measured their blood concentration of beta-hydroxybutyrate (BHB) and glucose twice daily using a handheld glucometer (Freestyle Precision Neo, Abbott, Chicago, IL, USA), and recorded their values in a provided protocol. In addition, values were stored on the device and read out later in the study center, providing an objective measure of compliance.

Fecal metagenomic sequencing

DNA isolation

DNA was isolated using ZymoBIOMICS DNA Miniprep Kit (ZymoReseach Europe GmbH, Freiburg, Germany). In short, an aliquot of 250 μ L of stool sample from the OMNIgene Gut tube was added to a ZR BasingBead Lysis Tube. The following extraction was done according to the manufacturer's instructions. DNA was eluted in 100 μ L RNase/DNase-free water and collected in a 1.5 mL Eppendorf Tube. Total DNA concentration was measured using NanoDrop ND-1000 (Peqlab Biotechnologie GmbH, Erlangen, Germany). Isolated DNA was stored at - 80°C⁵².

Shotgun metagenomics

Isolated DNA was shipped on dry ice to Novogene (Cambridge, UK) for shotgun metagenomic DNA sequencing. In short, DNA was fragmented and subsequently underwent end repair and phosphorylation. After A-tailing, adapter ligation was performed. Then 150 bp paired-ending sequencing was performed on the Illumina Novaseq 6000 platform with an aimed data collection of 6Gb raw data.

Microbiome data processing

Sequencing reads were mapped to the mOTUv2 (version 2.6) database, and read counts were subsequently rarefied using the RTK R package (version 0.2.6.1) to standardize sequencing depth across samples. Rarefaction involves randomly subsampling reads to match the sample with the lowest read depth, thereby mitigating biases introduced by variable sequencing depth and enabling reliable comparisons across cohorts. For the LEANER (healthy) cohort, a cutoff of 3,859 reads was applied, resulting in the exclusion of one sample due to insufficient sequencing depth. The same threshold was used for the Maifeld cohort⁵, where one sample was also excluded. In the Bahr dataset¹⁷, applying the same rarefaction criteria led to the exclusion of one sample. This consistent approach enabled reliable comparisons across cohorts and increased the robustness of downstream analyses.

Plasma metabolomics

Collection of plasma

Venous blood was collected in Vacutainer® EDTA tubes (BD, Heidelberg, Germany) and immediately put on crushed ice for 30 min and then centrifuged (3,000 g, 4°C, 10 min).

Plasma was collected and stored at - 80°C.

525

526

527

528

529

530

531

532

533

534

535

536

537

538

539

540

541

542

543

544

545

546

547

Preparation of plasma for nuclear magnetic resonance spectroscopy (NMR) Plasma samples were prepared with a robotic system (SamplePro Tube, Bruker BioSpin GmbH, Ettlingen, Germany) by mixing 287 µL plasma with 287 µL IVDr buffer (Bruker BioSpin GmbH, Ettlingen, Germany) and adding 10 µL formic acid (240 mM) as internal standard. NMR measurement of plasma All NMR experiments were performed on a 600 MHz Bruker Avance III spectrometer, using a triple resonance (¹H, ¹³C, ¹⁵N, ²H lock) helium cooled cryoprobe with z-gradient. Samples were handled by an automatic Bruker SampleJet sample changer (Bruker Biospin GmbH, Ettlingen, Germany). Tuning and matching of the probe as well as locking and shimming of the sample were performed automatically. Following the Bruker IVDr protocol for plasma measurements, for each sample four different types of ¹H NMR spectra were acquired at 310 K (1D NOESY, 2D JRES, 1D CPMG, and 1D spin echo diffusion spectrum). Data analysis of plasma NMR spectra From the collected spectra of each specimen, 41 smaller, non-lipoprotein metabolites were automatically identified and quantified using the Bruker IVDr Quantification in Plasma/Serum B.I.Quant-PSTM platform. Of note, only metabolites levels not bound to proteins were determined. Additionally, 112 lipoprotein parameters including various lipoprotein fractions, classes and subfractions were identified and quantified using the Bruker IVDr Lipoprotein Subclass Analysis B.I.LISATM platform. Stool metabolomics Drying of stool samples

Fecal samples from OMNImet Gut tubes were processed for metabolomics. Fecal samples (1 mL) were dissociated two times after adding 2.5 mL 70% isopropanol using C tubes with the gentleMACS OctoDissociator (Miltenyi Biotec, Bergisch Gladbach, Germany). Aliquots of dissociated samples were covered with perforated Parafilm and dried overnight in a vacuum concentrator (Concentrator 5301, Eppendorf, Hamburg, Germany). Dried samples were stored at - 80°C.

Preparation of stool for NMR

Dried stool samples were resuspended in 600 μ L (< 10 mg dry weight), 800 μ L (10-40 mg dry weight) or 1,000 μ L (> 40 mg dry weight) of double distilled water and 10 μ L of an extraction standard (Nicotinic acid at 80 mmol/L) were added. Samples were centrifuged three times (12 000 x g, 4 °C, 10 min) and supernatants were transferred into a fresh vial after each centrifugation in order to remove particles. Of the final supernatant, 400 μ L were mixed with 200 μ L of 0.1 mol/L phosphate buffer (pH 7.4) and 50 μ L of a 0.75% (w/v) solution of 3-trimethylsilyl-2,2,3,3-tetradeuteropropionate (TSP; Sigma-Aldrich, Taufkirchen, Germany), which served as an internal standard, in deuterium oxide.

NMR measurements of stool

NMR experiments were conducted on the same NMR spectrometer as described for the plasma analyses. Before measurement, each sample was allowed to equilibrate for 300 sec in the magnet, and the probe was automatically locked, tuned, matched, and shimmed. One-dimensional 1H NMR spectra were obtained at 298 K using a nuclear Overhauser enhancement spectroscopy pulse sequence with solvent signal suppression by pre-saturation during relaxation and mixing time. For each spectrum, 512 scans were collected into 65,536

573

574

575

576

577

578

579

580

581

582

583

584

585

586

587

588

589

590

591

592

593

594

595

data points over a 20-ppm (parts/million) spectral width using a relaxation delay of 4 sec, an acquisition time of 2.66 sec, and a mixing time of 0.01 sec. Spectra were automatically Fourier transformed and phase and baseline corrected. Data analysis of stool NMR spectra In each spectrum, a set of 41 metabolites were semi-automatically identified and relative to the TSP reference signal quantified using the CHENOMX 9.02 (Chenomx Inc, Edmonton, Canada) software suite. To account of potential losses during sample preparation resulting data was adjusted to the extraction standard and normalized to dry weight. Statistical analysis Descriptive statistics for interval variables are presented as mean ± standard deviation or median with interquartile range (IQR). For comparisons of delta BMI between responders and non-responders, normality of variable distributions was assessed by visual check of histograms and qq-plots. Mann-Whitney U-test or T-test was used as appropriate. For all other data, comparisons between independent groups were performed using the Mann-Whitney U test, and paired samples were compared using the Wilcoxon signed-rank test. Where applicable, p-values were adjusted for multiple comparisons using either the Holm method (for family-wise error control) or the Benjamini-Hochberg (BH) procedure (for false discovery rate control), depending on the analytical objective. Permutational Multivariate Analysis of Variance (PERMANOVA) was used to test for multivariate compositional differences between groups and visits. To evaluate the relationship between bacterial abundance and metabolite concentrations

while accounting for visit timepoint, we performed permutation-based conditional

independence tests. Specifically, for each metabolite, its association with Oscillibacter sp. 57_20 and Faecalibacterium sp. incertae sedis was tested while conditioning on the visit variable, using the R package coin (version 1.4.3) with 10,000 permutations. Resulting p-values were corrected for multiple testing using the Benjamini-Hochberg false discovery rate (FDR) method. Statistical significance was defined as p < 0.05 or q < 0.1, where applicable.

Data and code availability

602

603

604

605

606

607

608

609

610

611

612

613

614

615

616

617

618

619

620

621

622

623

624

All code, data, and scripts used in this study have been made publicly available. The code, scripts and processed raw data can be accessed on Zenodo (doi: https://doi.org/10.5281/zenodo.15696891). Raw sequencing data will be deposited in the NCBI database upon publication.

Acknowledgement

We would like to thank Anja Mähler for designing and setting up the LEANER study, for recruiting the study cohort, the entire study organization and establishing the network around this fasting study. We thank Alexandra Prüß who assisted as a fasting guide in carrying out study protocols. We thank Jana Czychi for her excellent technical assistance. This work was funded by intramural funds of the Experimental and Clinical Research Center, a cooperation between the Max Delbrück Center for Molecular Medicine in the Helmholtz Association and Charité - Universitätsmedizin Berlin; and external funds from the Karl and Veronica Carstens foundation (KVC 0/120/2021). FP, NW, HB, DNM, WG and PJO were supported by the BMFTR (Federal Ministry of Research, Technology and Space), project IDs 01EJ2202A, 01EJ2202D and 01EJ2202B (TAhRget consortium). FP, NW, and SKF were supported by the European union (HORIZON-HLTH-2022-STAYHLTH-02, IMMEDIATE consortium). TUPB was supported by the Berlin Center for Translational Vascular Biomedicine, jointly founded by BIH, Charité - Universitätsmedizin, and the Max Delbrück Center. DNM and NW were supported by the DZGIF (DZG Innovation Fund), Topic "Microbiome". SKF, DNM and NW were supported by the German Research Foundation (DFG), project ID 437531118 (CRC1470, projects A05, A06 and A10). SKF was

626

627

628

629

630

631

632

633

634

635

636

637

638

639

640

641

supported by the DFG project TRR412 and DZHK. AZ was was supported by the DFG, project ID 324392634 (TR221). **Author Contributions** CRediT: Conceptualization: TUPB, SB, HB, NS; Data curation: GNK, TUPB, LSB, FG, SB, HB; Formal Analysis: GNK, TUPB, UL, MM, AK, HB; Funding acquisition: TUPB, NW, PO, WG, DNM, SKF, SB, HB, NS; Investigation: KK, TS, SK, GR, VM, LB, LM, LSB, FG, FP, SB, NS; Methodology: GNK, TUPB, UL, WG, PJO, SKF, HB; Project administration: SB, HB, NS; Resources: NW, AZ, PO, WG, DNM, SKF, SB, HB, NS; Software: GNK, TUPB, UL, AK, SKF; Supervision: TUPB, UL, AZ, PO, WG, DNM, SKF, SB, HB, NS; Validation: GNK, TUPB, LSB, FG, FP, HB; Visualization: GNK, TUPB, HB; Writing – original draft: GNK, TUPB, SB, HB, NS; Writing – review & editing: GNK, TUPB, KK, TS, SK, UL, GR, VM, LB, LM, MM, AK, LSB, FG, FP, NW, AZ, PO, WG, DNM, SKF, SB, HB, NS. **Conflict of interest** NS has received speaker honoraria from Teva GmbH, Alexion Pharma Germany GmbH and Roche Pharma AG. The other authors declare no competing interests.

Tables

Table 1. Baseline characteristics of healthy participants depending on their randomization to fasting and waiting control arm. Data are given as means (SD). p-values fasting vs. waiting by t-test. BMI, body mass index; eGFR, estimated glomerular filtration rate; ALT, alanine aminotransferase; TSH, thyroid-stimulating hormone; CRP, C-reactive protein; HbA1c, glycated hemoglobin.

Variable	All	Fasting	Waiting	<i>P</i> value
Number (n)	38	19	19	
Sex, female	19 / 38 (50%)	9 / 19 (47%)	10 / 19 (53%)	>0.9
Age (years)	38 (8)	39 (9)	36 (8)	0.4
BMI (kg/m²)	25.1 (2.5)	25.0 (2.7)	25.2 (2.3)	0.7
eGFR (ml/min/1.73 m²)	102 (14)	98 (12)	106 (15)	0.1
ALT (U/I)	23.1 (8.1)	23.0 (8.2)	23.2 (8.2)	0.2
TSH (mU/l)	1.70 (0.84)	1.77 (0.91)	1.64 (0.77)	0.6
CRP (mg/dl)	0.98 (0.87)	0.78 (0.28)	1.17 (1.17)	0.2
Cholesterol (mg/dl)	182 (36)	189 (35)	175 (36)	0.2
HbA1c (mmol/mol)	33.2 (2.8)	34.2 (2.6)	32.3 (2.7)	0.03
Hemoglobin (g/dl)	14.0 (1.3)	13.8 (1.3)	14.2 (1.2)	0.41
White blood count (uL ⁻¹)	5.46 (1.02)	5.56 (0.96)	5.37 (1.09)	0.6
Thrombocytes (uL ⁻¹)	240 (42)	238 (63)	239 (54)	0.9

Figure Legends

649

650

651

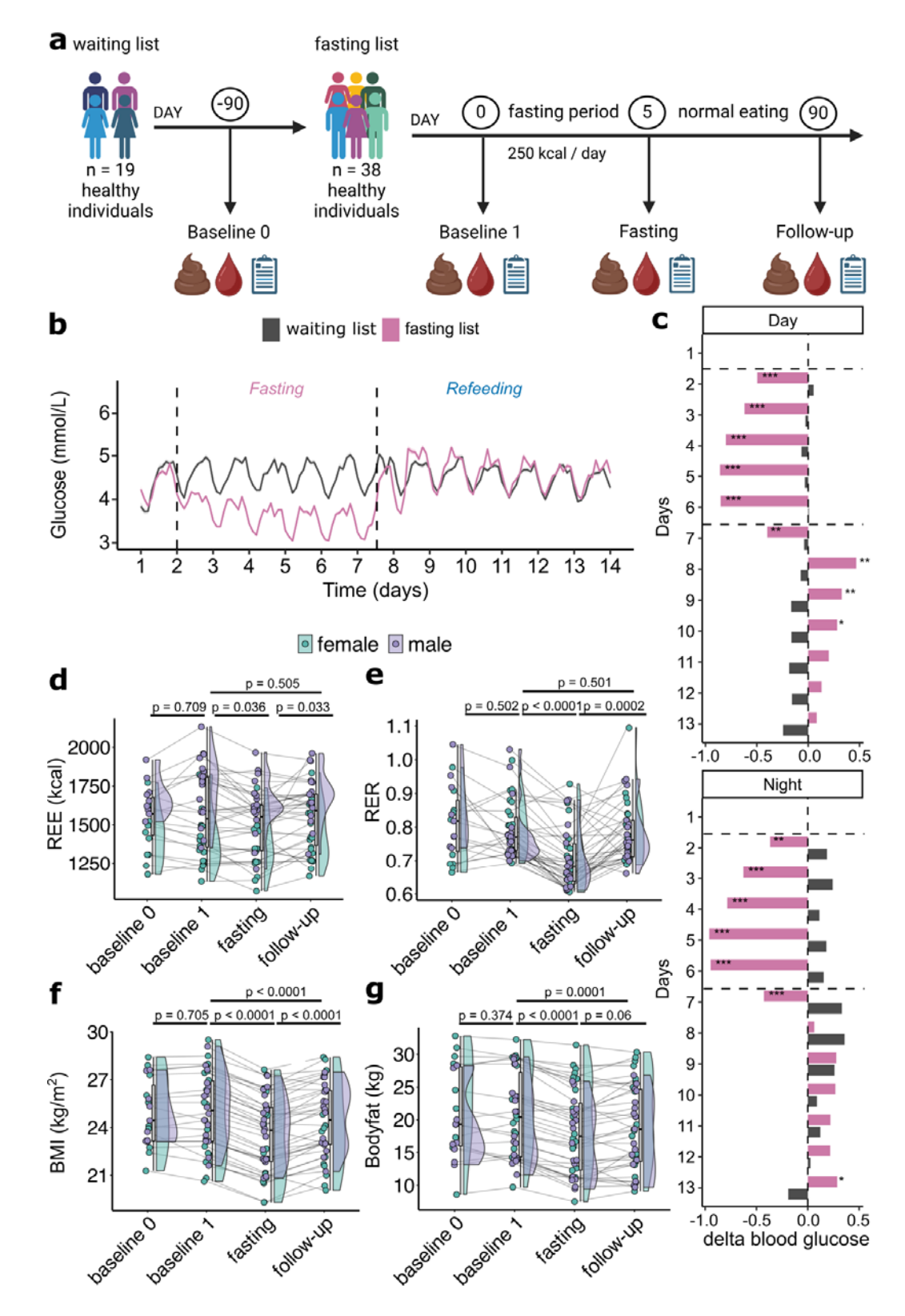


Figure 1. Physiological effects of prolonged fasting in healthy individuals. a) Schematic overview of the randomized waitlist-controlled trial. A total of 38 healthy participants were

654

655

656

657

658

659

660

661

662

663

664

665

666

667

668

669

670

recruited. The first 19 participants immediately underwent prolonged fasting, while the remaining 19 served as a waitlist control group. After the initial intervention period, the waitlist group also underwent the same prolonged fasting protocol, resulting in a complete dataset of 38 participants undergoing prolonged fasting. The fasting intervention consisted of a 5-day period with 250 kcal/day, preceded and followed by baseline and follow-up visits at days 0, 5, and 90. Stool, blood, and clinical data were collected at each visit. The waitlist group was assessed at an additional baseline (day -90) to control for temporal fluctuations. b) Glucose time series measured by continuous intradermal monitoring starting one day prior to fasting (pink) or at baseline for the waiting list control (grey). c) Quantification of absolute changes in mmol/L during the mean daytime (6am to 10pm) glucose levels (top) and night (10pm to 6am) glucose levels (bottom) as changes compared to the individual baseline (day 1). Paired t-test with Benjamini-Hochberg false discovery rate correction (BH-FDR), *q<0.1, **q<0.01, ***q<0.001. **d)** Resting energy expenditure (REE), **e)** respiratory exchange ratio (RER), f) body mass index (BMI), and g) body fat percentage at the different study visits. Each point represents one participant, lines connect individuals, boxplot (middle) for all participants, violins (right side) and dots coloured by sex. P-values are from Wilcoxon signed-rank tests and were corrected using the Holm method.

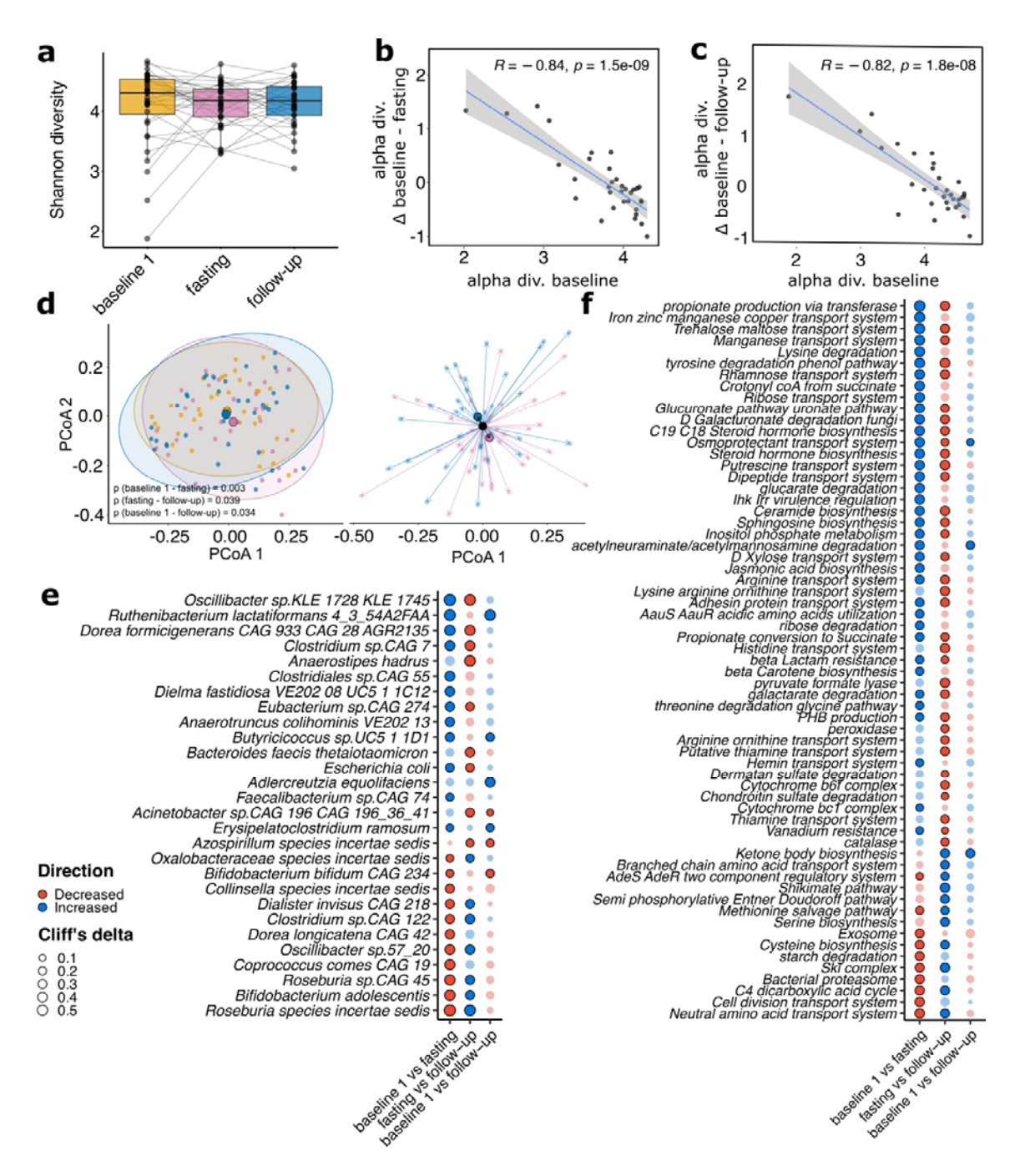
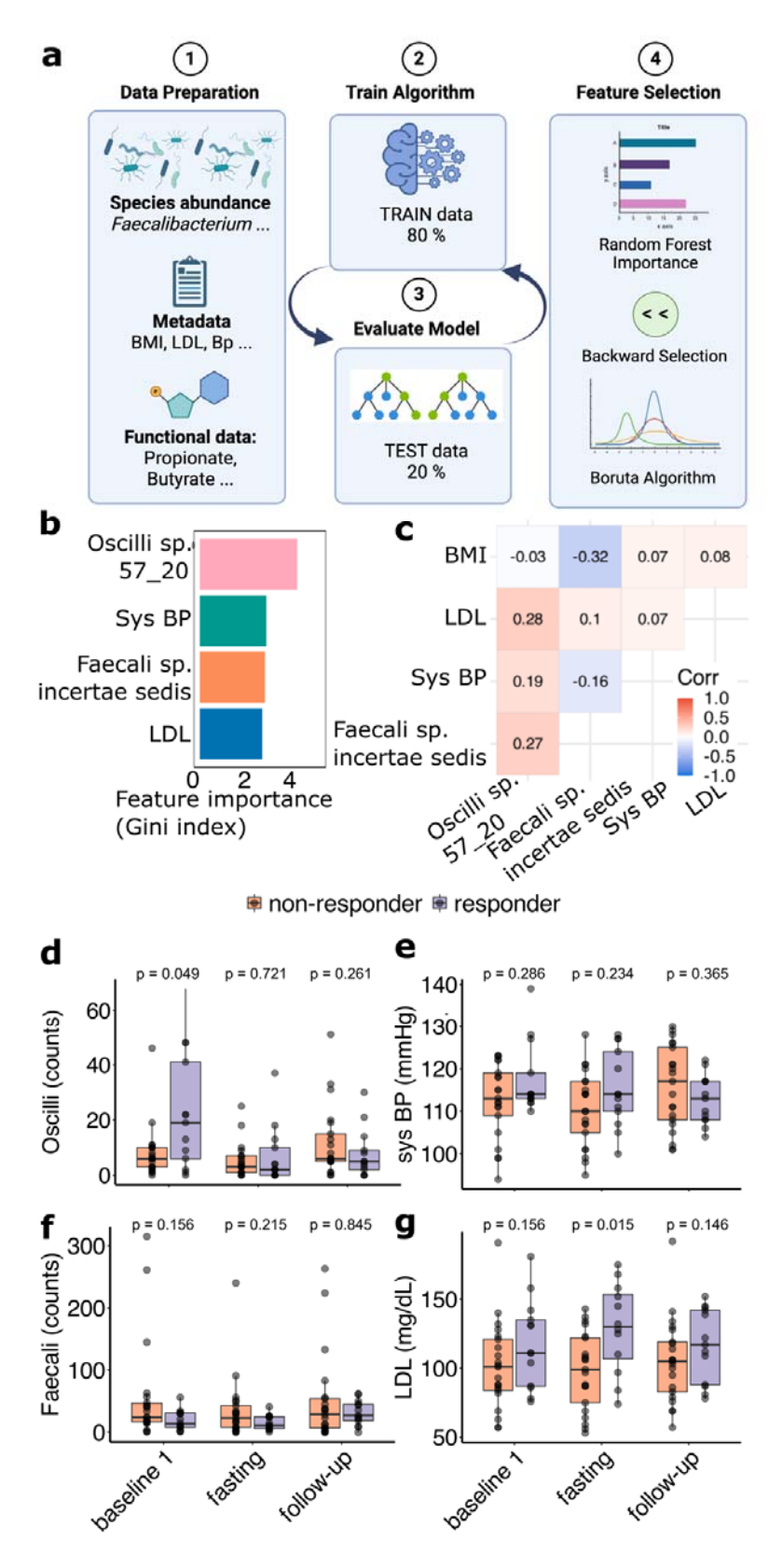


Figure 2. Prolonged fasting induces transient alterations in gut microbiome composition and function. a) Alpha diversity as measured by Shannon index for the study visits. Correlation of Shannon index at baseline with changes in Shannon index immediately b) post-fasting and c) at 12-week follow-up, indicating that baseline diversity predicts microbiome responsiveness. d) Principal coordinate analysis (PCoA) based on Bray-Curtis dissimilarity (naïve, left) and centered on baseline visit for fasting effect and on fasting visit

for post-fasting effect (right) show a transient shift in overall microbial composition after fasting (pink), which partially reverts at follow-up (blue). Ellipses represent 95% confidence intervals p-values from PERMANOVA. Dot plots showing differential abundant **e)** species (taxonomic level) and **f)** gut metabolic modules (functional level). Dots show fasting effects, follow-up effects and study effects, transparency indicates non-significant findings (q>0.1), dot size shows absolute Cliff's delta, color shows directionality. Significance by Wilcoxon signed-rank test with Benjamini–Hochberg false discovery rate correction.



687

Figure 3. Machine learning model predicts sustained BMI response to prolonged fasting using clinical and microbiome features. a) Schematic overview of the multi-omics feature

selection and classification pipeline. Baseline species abundances, clinical metadata, and functional modules were used to train a random forest classifier. Important features were selected through recursive feature elimination, Boruta algorithm, and backward selection. b) Final model includes four top-ranked features: Faecalibacterium sp. incertae sedis, Oscillibacter sp. 57_20, LDL cholesterol, and systolic blood pressure. c) Correlation heatmap of the selected features showing independence from baseline BMI. R-values from Spearman correlation d) Boxplots of the four selected features at baseline, comparing BMI responders and non-responders, dots show individual patients. P-values by Mann-Whitney-U-test. Oscilli, Oscillibacter sp. 57_20; Faecali, Faecalibacterium sp. incertae sedis; LDL, Low-density lipoprotein cholesterol; sys BP, systolic blood pressure.

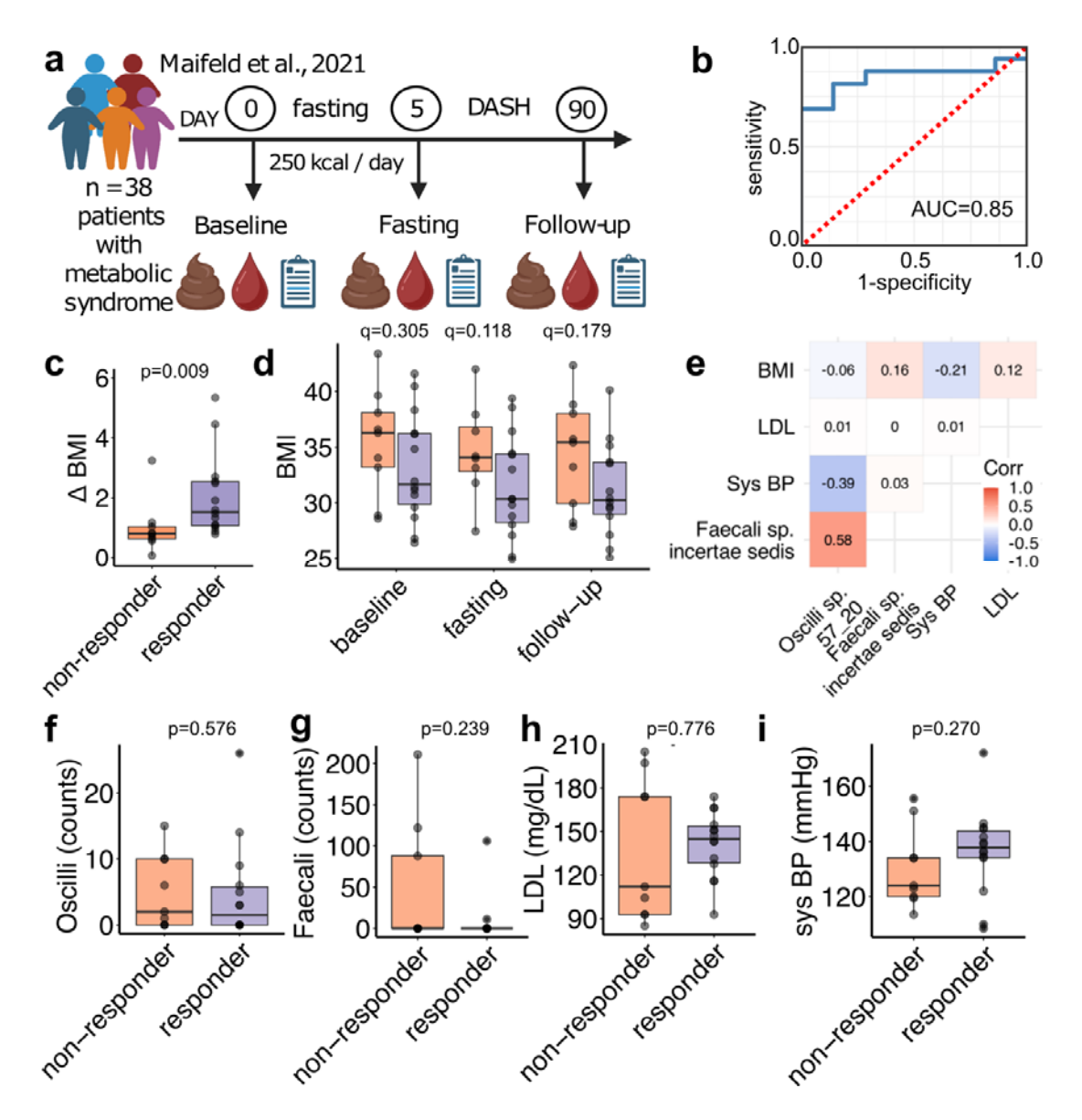


Figure 4. Validation of BMI response prediction model in a fasting cohort of patients with metabolic syndrome. a) Schematic of the Maifeld et al. (2021) study: 5-day fasting followed by a DASH diet in individuals with metabolic syndrome (n = 38), with BMI follow-up after 12 weeks. b) Receiver operating characteristic (ROC) curve of model performance in the Maifeld cohort, showing good predictive accuracy (AUC = 0.85). c) BMI reduction at follow-up of patients classified as responder or non-responder by the prediction model. p-value by one-tailed unpaired t-test. d) BMI over the course of the study, split by participants classified as responders or non-responders. Each point represents a participant. P-values are from paired

Wilcoxon signed-rank tests and were corrected for multiple comparisons using the Benjamini-Hochberg false discovery rate (FDR-BH) method. e) Correlation heatmap of model features (*Oscillibacter sp. 57_20*, *Faecalibacterium sp.* incertae sedis, LDL, systolic blood pressure) within the Maifeld dataset. Features used for classification at baseline: f) *Oscillibacter sp. 57_20*, g) *Faecalibacterium sp.* incertae sedis, h) LDL, and i) systolic blood pressure. Oscilli, *Oscillibacter sp. 57_20*; Faecali, *Faecalibacterium sp.* incertae sedis; LDL, Low-density lipoprotein cholesterol; sys BP, systolic blood pressure.

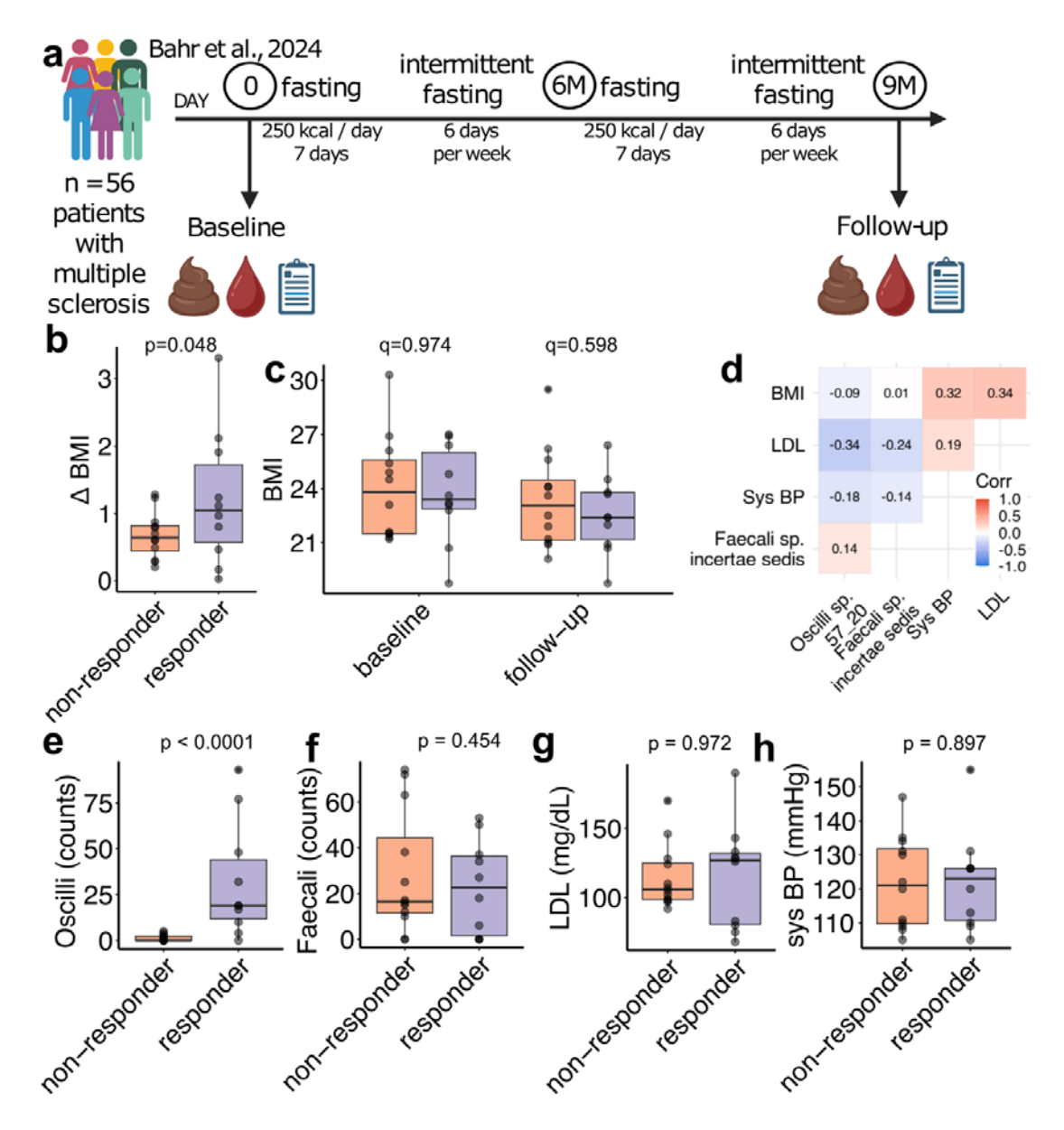


Figure 5. Validation of BMI response prediction model in a fasting cohort of patients with multiple sclerosis. a) Schematic of the Bahr et al. (2024) study: two 7-day fasting periods and intermittent fasting in individuals with multiple sclerosis (n = 56), over a 9-month period. b) BMI reduction at follow-up of patients classified as responder or non-responder by the prediction model. p-value by one-tailed unpaired t-test. c) BMI reduction at follow-up of patients classified as responder or non-responder by the prediction model. p-value by one-tailed unpaired t-test. d) BMI over the course of the study, split by participants classified as responders or non-responders. Each point represents a participant. P-values are from paired

Wilcoxon signed-rank tests and were corrected for multiple comparisons using the Benjamini-Hochberg false discovery rate (FDR-BH) method. d) Correlation matrix of selected features in the Bahr dataset. Features used for classification at baseline: f) Oscillibacter sp. 57_20, g) Faecalibacterium sp. incertae sedis, h) LDL, and i) systolic blood pressure. Oscilli, Oscillibacter sp. 57_20; Faecali, Faecalibacterium sp. incertae sedis; LDL, Low-density lipoprotein cholesterol; sys BP, systolic blood pressure.

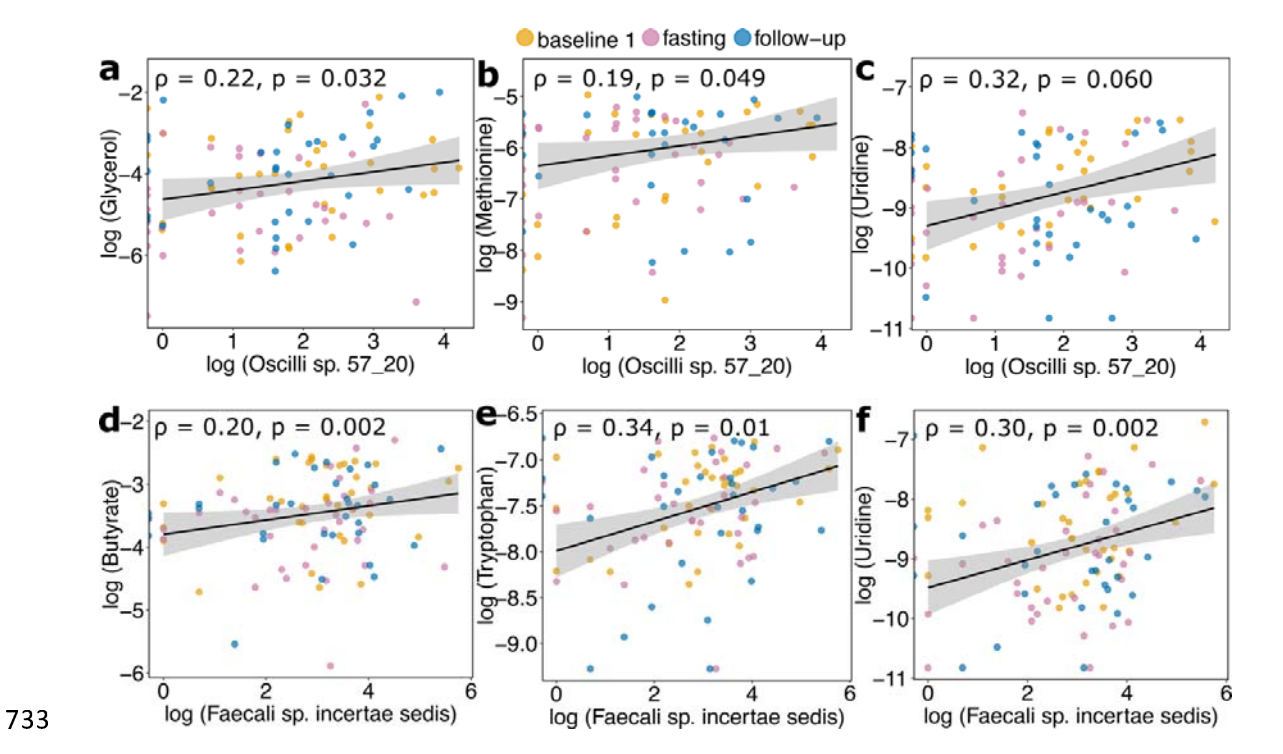


Figure 6. Oscillibacter sp. 57_20 and Faecalibacterium sp. incertae sedis abundance correlates with fecal metabolome. Correlation of Oscillibacter (Oscilli) sp. 57_20 abundance with fecal a) glycerol, b) methionine, and c) uridine levels. Correlation of Faecalibacterium (Faecali) sp. incertae sedis abundance with fecal d) butyrate, e) tryptophan, and f) uridine levels. R-values from Spearman's correlation. P-values from permutation-based independence test screening for associations of species with metabolites while blocking effects of study visits. Abbreviations: Oscilli: Oscillibacter sp. 57_20; Faecali: Faecalibacterium sp. incertae sedis.

743 References 744 Di Francesco, A., Di Germanio, C., Bernier, M. & de Cabo, R. A time to fast. Science 1 745 **362**, 770-775 (2018). https://doi.org:10.1126/science.aau2095 746 2 Brandhorst, S. et al. Fasting-mimicking diet causes hepatic and blood markers changes 747 indicating reduced biological age and disease risk. Nat Commun 15, 1309 (2024). 748 https://doi.org:10.1038/s41467-024-45260-9 749 Gewecke, K. et al. Long-term fasting induces a remodelling of fatty acid composition 3 750 in erythrocyte membranes. Eur J Clin Invest, e14382 (2025). 751 https://doi.org:10.1111/eci.14382 752 Koppold, D. A. et al. International consensus on fasting terminology. Cell Metab 36, 753 1779-1794 e1774 (2024). https://doi.org:10.1016/j.cmet.2024.06.013 754 5 Maifeld, A. et al. Fasting alters the gut microbiome reducing blood pressure and body 755 weight in metabolic syndrome patients. Nat Commun 12, 1970 (2021). 756 https://doi.org:10.1038/s41467-021-22097-0 757 6 Cignarella, F. et al. Intermittent Fasting Confers Protection in CNS Autoimmunity by 758 Altering the Gut Microbiota. Cell Metab 27, 1222-1235 e1226 (2018). 759 https://doi.org:10.1016/j.cmet.2018.05.006 7 760 Choi, I. Y. et al. A Diet Mimicking Fasting Promotes Regeneration and Reduces 761 Autoimmunity and Multiple Sclerosis Symptoms. Cell Rep 15, 2136-2146 (2016). 762 https://doi.org:10.1016/j.celrep.2016.05.009 763 8 de Groot, S. et al. Fasting mimicking diet as an adjunct to neoadjuvant chemotherapy 764 for breast cancer in the multicentre randomized phase 2 DIRECT trial. Nat Commun 765 **11**, 3083 (2020). https://doi.org:10.1038/s41467-020-16138-3 766 9 Ratiner, K., Ciocan, D., Abdeen, S. K. & Elinav, E. Utilization of the microbiome in 767 personalized medicine. Nat Rev Microbiol 22, 291-308 (2024). 768 https://doi.org:10.1038/s41579-023-00998-9 769 10 von Schwartzenberg, R. J. et al. Caloric restriction disrupts the microbiota and 770 colonization resistance. Nature 595, 272-277 (2021). https://doi.org:10.1038/s41586-771 021-03663-4 772 Murthy, V. L. et al. Metabolic liability for weight gain in early adulthood. Cell Rep Med 11 773 5, 101548 (2024). https://doi.org:10.1016/j.xcrm.2024.101548

774	12	Jiang, Z. et al. Human gut microbial aromatic amino acid and related metabolites
775		prevent obesity through intestinal immune control. Nat Metab 7, 808-822 (2025).
776		https://doi.org:10.1038/s42255-025-01246-5
777	13	Hill, D. A. et al. Metagenomic analyses reveal antibiotic-induced temporal and spatial
778		changes in intestinal microbiota with associated alterations in immune cell
779		homeostasis. Mucosal Immunol 3, 148-158 (2010).
780		https://doi.org:10.1038/mi.2009.132
781	14	Rakoff-Nahoum, S., Paglino, J., Eslami-Varzaneh, F., Edberg, S. & Medzhitov, R.
782		Recognition of commensal microflora by toll-like receptors is required for intestinal
783		homeostasis. Cell 118, 229-241 (2004). https://doi.org:10.1016/j.cell.2004.07.002
784	15	Zheng, J. et al. Noninvasive, microbiome-based diagnosis of inflammatory bowel
785		disease. Nat Med 30 , 3555-3567 (2024). https://doi.org:10.1038/s41591-024-03280-4
786	16	Ozarda, Y. et al. Protocol and standard operating procedures for common use in a
787		worldwide multicenter study on reference values. Clin Chem Lab Med 51 , 1027-1040
788		(2013). https://doi.org:10.1515/cclm-2013-0249
789	17	Bahr, L. S. et al. Fasting, ketogenic and anti-inflammatory diets stabilized active
790		relapsing-remitting multiple sclerosis over 18 months — a randomized, controlled
791		study. <i>medRxiv</i> , 2024.2008.2013.24311863 (2024).
792		https://doi.org:10.1101/2024.08.13.24311863
7 93	18	Hothorn, T., Hornik, K., van de Wiel, M. A. & Zeileis, A. Implementing a Class of
794		Permutation Tests: The coin Package. <i>Journal of Statistical Software</i> 28 , 1 - 23 (2008).
795		https://doi.org:10.18637/jss.v028.i08
796	19	Berry, S. E. et al. Human postprandial responses to food and potential for precision
797		nutrition. Nat Med 26, 964-973 (2020). https://doi.org:10.1038/s41591-020-0934-0
798	20	Zeevi, D. et al. Personalized Nutrition by Prediction of Glycemic Responses. Cell 163,
799		1079-1094 (2015). https://doi.org:10.1016/j.cell.2015.11.001
800	21	Horton, T. J. & Hill, J. O. Prolonged fasting significantly changes nutrient oxidation and
801		glucose tolerance after a normal mixed meal. J Appl Physiol (1985) 90, 155-163
802		(2001). https://doi.org:10.1152/jappl.2001.90.1.155
803	22	Solianik, R., Zidoniene, K., Eimantas, N. & Brazaitis, M. Prolonged fasting outperforms
804		short-term fasting in terms of glucose tolerance and insulin release: a randomised

		W. L I
805		controlled trial. <i>Br J Nutr</i> 130 , 1500-1509 (2023).
806		https://doi.org:10.1017/S0007114523000557
807	23	Laurens, C. et al. Is muscle and protein loss relevant in long-term fasting in healthy
808		men? A prospective trial on physiological adaptations. J Cachexia Sarcopenia Muscle
809		12, 1690-1703 (2021). https://doi.org:10.1002/jcsm.12766
810	24	Dai, Z. et al. Effects of 10-Day Complete Fasting on Physiological Homeostasis,
811		Nutrition and Health Markers in Male Adults. Nutrients 14 (2022).
812		https://doi.org:10.3390/nu14183860
813	25	Triffoni-Melo, A. T., Suen, V. M. M., Resende, C. M. M., Braga, C. B. M. & Diez-Garcia,
814		R. W. Resting energy expenditure adaptation after short-term caloric restriction in
815		morbidly obese women. Rev Nutr 28, 505-511 (2015). https://doi.org:10.1590/1415-
816		52732015000500005
817	26	Schlogl, M. et al. Energy Expenditure Responses to Fasting and Overfeeding Identify
818		Phenotypes Associated With Weight Change. <i>Diabetes</i> 64 , 3680-3689 (2015).
819		https://doi.org:10.2337/db15-0382
820	27	Mohr, A. E. et al. Gut microbiome remodeling and metabolomic profile improves in
821		response to protein pacing with intermittent fasting versus continuous caloric
822		restriction. Nat Commun 15, 4155 (2024). https://doi.org:10.1038/s41467-024-
823		<u>48355-5</u>
824	28	Ducarmon, Q. et al. Long-term fasting remodels gut microbial metabolism and host
825		metabolism. <i>bioRxiv</i> , 2024.2004.2019.590209 (2024).
826		https://doi.org:10.1101/2024.04.19.590209
827	29	Wang, Y. C. et al. Indole-3-Propionic Acid Protects Against Heart Failure With
828		Preserved Ejection Fraction. Circ Res 134, 371-389 (2024).
829		https://doi.org:10.1161/CIRCRESAHA.123.322381
830	30	Barcenilla, A. et al. Phylogenetic relationships of butyrate-producing bacteria from
831		the human gut. Appl Environ Microbiol 66, 1654-1661 (2000).
832		https://doi.org:10.1128/AEM.66.4.1654-1661.2000
833	31	Essex, M. et al. Gut microbiota dysbiosis is associated with altered tryptophan
834		metabolism and dysregulated inflammatory response in COVID-19. NPJ Biofilms
835		Microbiomes 10, 66 (2024). https://doi.org:10.1038/s41522-024-00538-0

836	32	Roager, H. M. & Licht, T. R. Microbial tryptophan catabolites in health and disease.
837		Nat Commun 9, 3294 (2018). https://doi.org:10.1038/s41467-018-05470-4
838	33	Hanssen, R. et al. Circulating uridine dynamically and adaptively regulates food intake
839		in humans. <i>Cell Rep Med</i> 4 , 100897 (2023).
840		https://doi.org:10.1016/j.xcrm.2022.100897
841	34	Deng, Y. et al. An adipo-biliary-uridine axis that regulates energy homeostasis. Science
842		355 (2017). https://doi.org:10.1126/science.aaf5375
843	35	Steculorum, S. M. et al. Hypothalamic UDP Increases in Obesity and Promotes
844		Feeding via P2Y6-Dependent Activation of AgRP Neurons. Cell 162, 1404-1417 (2015).
845		https://doi.org:10.1016/j.cell.2015.08.032
846	36	Deng, Y. et al. Adipocyte Xbp1s overexpression drives uridine production and reduces
847		obesity. Mol Metab 11, 1-17 (2018). https://doi.org:10.1016/j.molmet.2018.02.013
848	37	Han, H. et al. From gut microbiota to host appetite: gut microbiota-derived
849		metabolites as key regulators. <i>Microbiome</i> 9 , 162 (2021).
850		https://doi.org:10.1186/s40168-021-01093-y
851	38	Ali, I. et al. Ramadan Fasting Leads to Shifts in Human Gut Microbiota Structured by
852		Dietary Composition. Front Microbiol 12, 642999 (2021).
853		https://doi.org:10.3389/fmicb.2021.642999
854	39	Lopez-Siles, M., Duncan, S. H., Garcia-Gil, L. J. & Martinez-Medina, M.
855		Faecalibacterium prausnitzii: from microbiology to diagnostics and prognostics. ISME
856		J 11, 841-852 (2017). https://doi.org:10.1038/ismej.2016.176
857	40	Remely, M. et al. Increased gut microbiota diversity and abundance of
858		Faecalibacterium prausnitzii and Akkermansia after fasting: a pilot study. Wien Klin
859		Wochenschr 127, 394-398 (2015). https://doi.org:10.1007/s00508-015-0755-1
860	41	Guo, Y. et al. Intermittent Fasting Improves Cardiometabolic Risk Factors and Alters
861		Gut Microbiota in Metabolic Syndrome Patients. J Clin Endocrinol Metab 106, 64-79
862		(2021). https://doi.org:10.1210/clinem/dgaa644
863	42	Mesnage, R., Grundler, F., Schwiertz, A., Le Maho, Y. & Wilhelmi de Toledo, F. Changes
864		in human gut microbiota composition are linked to the energy metabolic switch
865		during 10 d of Buchinger fasting. J Nutr Sci 8, e36 (2019).
866		https://doi.org:10.1017/jns.2019.33

867	43	Ozkul, C., Yalinay, M. & Karakan, T. Structural changes in gut microbiome after
868		Ramadan fasting: a pilot study. Benef Microbes 11, 227-233 (2020).
869		https://doi.org:10.3920/BM2019.0039
870	44	Sinha, A. K. et al. Dietary fibre directs microbial tryptophan metabolism via metabolic
871		interactions in the gut microbiota. Nat Microbiol 9, 1964-1978 (2024).
872		https://doi.org:10.1038/s41564-024-01737-3
873	45	Fassarella, M. et al. Gut microbiome stability and resilience: elucidating the response
874		to perturbations in order to modulate gut health. Gut 70, 595-605 (2021).
875		https://doi.org:10.1136/gutjnl-2020-321747
876	46	Khan, M. N. et al. Intermittent fasting positively modulates human gut microbial
877		diversity and ameliorates blood lipid profile. Front Microbiol 13, 922727 (2022).
878		https://doi.org:10.3389/fmicb.2022.922727
879	47	Rajput, D., Wang, W. J. & Chen, C. C. Evaluation of a decided sample size in machine
880		learning applications. BMC Bioinformatics 24, 48 (2023).
881		https://doi.org:10.1186/s12859-023-05156-9
882	48	Birkenbihl, C. et al. Differences in cohort study data affect external validation of
883		artificial intelligence models for predictive diagnostics of dementia - lessons for
884		translation into clinical practice. EPMA J 11, 367-376 (2020).
885		https://doi.org:10.1007/s13167-020-00216-z
886	49	Harris, P. A. et al. The REDCap consortium: Building an international community of
887		software platform partners. J Biomed Inform 95, 103 208 (2019).
888		https://doi.org:10.1016/j.jbi.2019.103208
889	50	Harris, P. A. et al. Research electronic data capture (REDCap)a metadata-driven
890		methodology and workflow process for providing translational research informatics
891		support. <i>J Biomed Inform</i> 42 , 377-381 (2009).
892		https://doi.org:10.1016/j.jbi.2008.08.010
893	51	Mahler, A. et al. Increased Salt Intake Decreases Diet-Induced Thermogenesis in
894		Healthy Volunteers: A Randomized Placebo-Controlled Study. Nutrients 14 (2022).
895		https://doi.org:10.3390/nu14020253
896	52	Bartolomaeus, T. U. P. et al. Quantifying technical confounders in microbiome studies.
897		Cardiovasc Res 117, 863-875 (2021). https://doi.org:10.1093/cvr/cvaa128
898		